

---

# A new approach to modelling structural responses to earthquakes

*H. Xu, X. Qin, N. Chow, T. Larkin & H.M. Osinga*

The University of Auckland, New Zealand.

## ABSTRACT

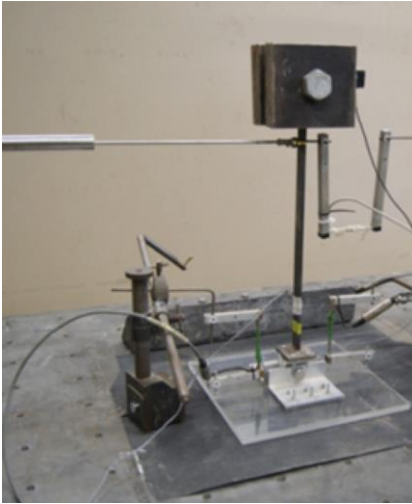
It is very difficult to model analytically the response of a structure under earthquake excitation. The conventional harmonic equation of motion is a linear model subjected to a load defined as the product of the mass of the structure and the ground acceleration. Shake table tests on a model structure using three different earthquake excitations were conducted. There is a significant difference between the responses generated from the classical linear model and the experimental measurements. Our hypothesis is that the load experienced by the structure is actually different from the load generated by the ground acceleration. We investigate possible adjustments to the load applied in the linear model based on the resonance frequency and the power spectrum of the measured responses. Our results indicate that successful adjustments can be made, so that the linear model generates a better approximation to the actual structural response.

## 1 INTRODUCTION

The structural response to an earthquake is notoriously hard to predict and structural damage is still an accepted consequence of when an earthquake strikes. Even the most advanced building designs cannot avoid structural failure when subjected to strong earthquakes (Chow, 1996; Chow & Hao, 2012; Kawashima et al., 2011; Orense et al., 2014), but damage can also occur at milder ground excitations, despite major efforts to understand such soil-structure interactions. The international workshop “Seismic Performance of Soil-Foundation-Structure (SFS) systems,” held at The University of Auckland in November 2016 (Chow et al., 2017), focussed particularly on facilitating communication between geotechnical and structural engineers, in a bid to gain a better understanding of the compound effects between the movements of soil and structure. The goal was to explain the underlying mechanisms and then quantify the effects of such SFS interactions. However, there is already an issue with the assumed load exerted on the structure. The classical view is to consider the structure as rigid, which means that the load exerted at the top of an SDOF structure is the same as at its base, and it is further assumed that this load is defined as the product of the mass of the structure and the ground acceleration,

which is supposed to be given (Chopra, 2001). Indeed, this is a fundamental modelling assumption that directly influences the predictable power of a theoretical analysis.

What is the precise load exerted on the structure? There are different ways to measure the load at the base of a structure and experimental results suggest that the classical view of structural mass times ground acceleration is not correct; see also (Qin et al., 2018) in this volume. This paper considers the hypothesis that the force exerted at the top of the SDOF structure is different from that exerted at its base, and it is this discrepancy that causes the error between experimental measurements and computed results from the theoretical equation. Here, we address the inverse problem of finding a correction to the load in the theoretical equation, that is, the identification problem of determining the system parameters when given the input and output (Crisp et al., 1990).



	System parameters	Unit
mass:	$m = 10$	kg
damping ratio:	$\zeta = 0.083$	
stiffness:	$k = 1.62$	kN / m
damping:	$c = 21.13$	N s / m

Figure 1: Experimental set-up of the inverted pendulum with mass 10 kg and height 425 mm; the pendulum is mounted on a fixed base of size 280 mm  $\times$  230 mm.

This paper reports on the analysis of the experiment of a mass on a (near massless) supporting structure that is subjected to three different excitations. Figure 1 shows the experimental set-up with mass  $m = 10$  kg and centre of mass at height 425 mm positioned on a fixed base of size 280 mm  $\times$  230 mm. The fundamental frequency was measured as  $f_F = 1.97$  Hz and the damping ratio was  $\zeta = 8.3$  %, respectively. Three different ground accelerations were applied, and measurements were taken at 5 ms intervals of the relative displacement  $u^{meas}$  and the corresponding acceleration  $\ddot{u}^{meas}$ .

The measured displacement  $u^{meas}$  of this SDOF structure is compared with the relative displacement  $u$  generated by the idealised theoretical equation, a (linear) harmonic oscillator forced by the product of the mass and the applied ground acceleration. The equation is then given by

$$m \ddot{u} + c \dot{u} + k u = -P(t), \quad (1)$$

where  $k$  is the stiffness or spring constant, estimated as 1.62 kN / m, the viscous damping coefficient  $c = 2\zeta\sqrt{m k}$  is estimated as 21.13 N s / m, and  $P(t) = m g \ddot{u}_g$  is the load (in Newton) generated by the ground acceleration  $\ddot{u}_g$ , which is measured in g. Equation (1) generates the relative displacement  $u$  in metres, but the experimental measurements are in millimetres; all figures show the displacement in the unit mm.

Equation (1) is only an approximate mathematical model, and it is expected that there is a difference between  $u$  and  $u^{meas}$ . The goal in this paper is to find simple corrections to Equation (1), such that  $|u - u^{meas}|$  is significantly decreased. The difference between the load experienced by the structure and the load generated by the earthquake may be intrinsic to the structure itself, or its origins could be that the load applied by the actuators during the experiment is not the same as the intended load. Rather than include a nonlinear correction to, say, the stiffness coefficient or other structure-dependent terms on the left-hand side of Equation (1), our intention is to apply a correction to its right-hand side.

## 2 COMPARING EXPERIMENT AND EQUATION

Three different ground accelerations were applied, of which the first is reported on in detail. Figure 2 shows the resulting measured displacement  $u^{meas}$  (green) as a function of time  $t$  in panel (a). Panel (b) shows the corresponding relative displacement  $u$  (blue) versus time  $t$ , which was generated by numerical integration of Equation (1) over the time interval  $[0, 24]$ . Overlaid is the applied ground acceleration  $\ddot{u}_g$  (grey), corresponding to the vertical axis on the right in both panels. There are two obvious differences between the responses  $u$  and  $u^{meas}$ : the maximum displacement for  $u$  is substantially larger than for  $u^{meas}$  (8.92 mm and 5.26 mm,



respectively); and the amplitude envelopes are quite different, particularly for  $10 \leq t \leq 15$ . Indeed, the difference in power or energy of the responses, defined as

$$E(u) := \int_0^{24} |u(t)|^2 dt \approx 125.21 \text{ mm}^2 \text{ s} \quad \text{and}$$

$$E(u^{meas}) := \int_0^{24} |u^{meas}(t)|^2 dt \approx 61.94 \text{ mm}^2 \text{ s},$$

is of the same order of magnitude as the responses themselves! This is a clear indication that the approximation error of Equation (1) is likely of first rather than higher order.

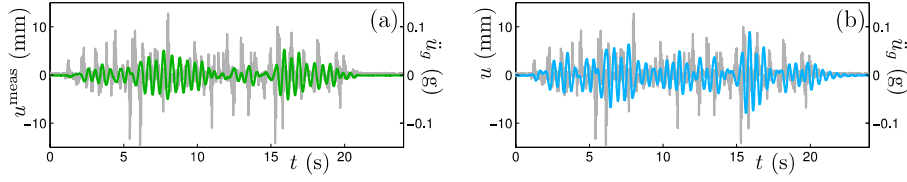


Figure 2: Measured and computed relative displacements  $u^{meas}$  (green) and  $u$  (blue) versus time  $t$ , shown in panels (a) and (b), respectively, together with the applied ground acceleration  $\ddot{u}_g$  (grey, measured in g).

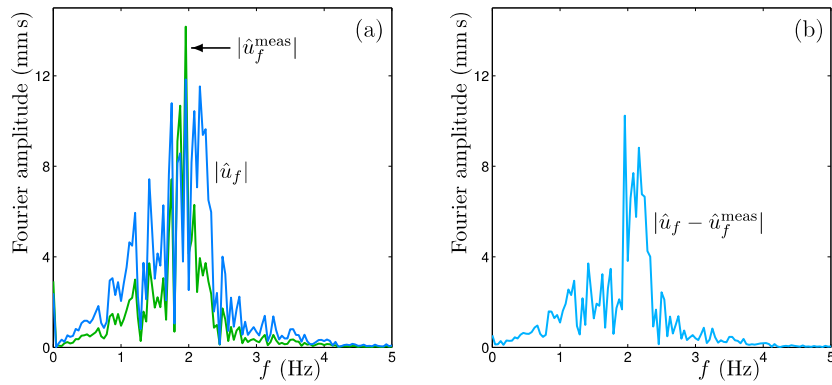


Figure 3: Power spectrum of the measured and computed relative displacements versus frequency  $f$  in Hz. Panel-(a) shows the modulus of the respective Fourier coefficients  $\hat{u}_f^{meas}$  (green) and  $\hat{u}_f$  (blue), and panel-(b) shows their difference  $|\hat{u}_f - \hat{u}_f^{meas}|$ .

The responses also exhibit significant differences when considered in the frequency domain. Figure 3 shows the Fourier amplitude  $|\hat{u}_f^{meas}|$  and  $|\hat{u}_f|$  of the Fourier transforms of the measured and computed responses  $u^{meas}$  and  $u$ , respectively. Their squares  $|\hat{u}_f^{meas}|^2$  and  $|\hat{u}_f|^2$  represent the respective power at each frequency. The horizontal axis shows only the frequencies  $f$  up to 5 Hz, because the power for the higher frequencies is almost 0. Both power spectra are shown in panel (a), while panel (b) shows the power spectrum of the difference  $|\hat{u}_f - \hat{u}_f^{meas}|$ . Note that the maxima for both  $|\hat{u}_f^{meas}|$  and  $|\hat{u}_f|$  (at are 14.17 mm s and 11.84 mm s, respectively) are achieved at  $f = 47/24 \approx 1.96$  Hz, which is the sampling frequency nearest to the fundamental frequency  $f_F$ . However, the power spectrum for  $\hat{u}$  is much broader around  $f_F$ ; this is more clearly seen when considering  $|\hat{u}_f - \hat{u}_f^{meas}|$ .

The total power can also be calculated from the power spectrum. For example,

$$E(u) = \int_0^{24} |u(t)|^2 dt = \int_{-100}^{100} |\hat{u}(f)|^2 df \approx \frac{1}{24} \sum_{i=0}^{100} |\hat{u}_f(i)|^2 \approx 125.21 \text{ mm}^2 \text{ s},$$

where  $n = 4800$  is the sampling size, and  $\hat{u}_f(i)$  is the Fourier coefficient associated with frequency  $f = i/24$ .

### 3 LINEAR CORRECTION

Equation (1) is supposed to approximate the true (relative) displacement to first order, but the experimental data suggests that this is not the case. As mentioned in the introduction, the cause of this discrepancy may be due to the fact that the SDOF structure experiences a different load than that resulting from the ground acceleration. In fact, it is likely that the actual load applied to the structure during the experiment is already different from the intended load due to the earthquake. However, there may be other effects that are intrinsic to the structure or due to the fact that Equation (1) assumes  $P(t) = m g \ddot{u}_g$ , even though  $P(t)$  is supposed to be the load that acts at the top of the SDOF structure, 425 mm above ground. We investigate the latter suggestion and attempt a linear correction of  $P(t)$  as follows. Consider Equation (1) with the adjusted right-hand side

$$m \ddot{u} + c \dot{u} + k u = -(1 - \gamma) P(t), \quad (2)$$



where  $\gamma$  is the correction parameter and the generated relative displacement  $u_\gamma$  depends on  $\gamma$ . Note that Equation (2) is still linear, which means that  $u_\gamma$  is proportional to the displacement  $u$  obtained from Equation (1). Recall that  $E(u) > E(u^{meas})$ . By using the total power  $E(u_\gamma - u^{meas})$  of the difference as a quantification of improvement, the goal is to find the value  $\gamma^*$  for  $\gamma$  that minimises  $E(u_\gamma - u^{meas})$ .

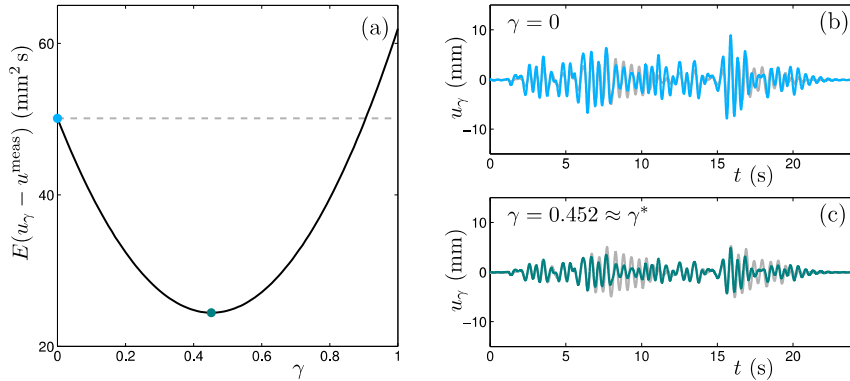


Figure 4: Improvement obtained by Equation (2) quantified in terms of the total power  $E(u_\gamma - u^{meas})$  of the difference with the measured displacement. Panel (a) shows that a value  $\gamma = \gamma^*$  exists that minimises  $E(u_\gamma - u^{meas})$  (teal dot). The original computed response  $u = u_\gamma$  with  $\gamma = 0$  is shown in blue versus  $t$  in panel (b), and the scaled response  $u = u_\gamma$  with  $\gamma = \gamma^*$  is shown in teal in panel (c); the measured displacement is also shown in grey in panels (b) and (c), for reference.

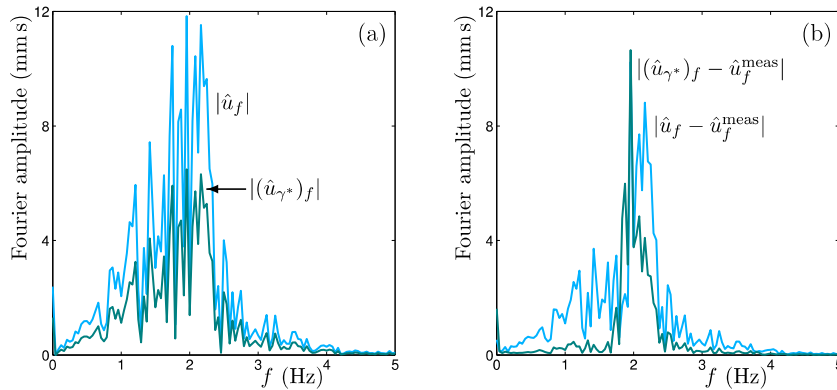


Figure 5: Power spectrum of the relative displacements computed with Equation (2) for  $\gamma = \gamma^*$ , denoted  $|(\hat{u}_{\gamma^*})_f|$  (teal), and computed with Equation (1), denoted  $|\hat{u}_f|$  (blue), versus frequency  $f$  in Hz in panel (a), and of their respective differences with the measured displacement, denoted  $|(\hat{u}_{\gamma^*})_f - \hat{u}_f^{meas}|$  (teal) and  $|\hat{u}_f - \hat{u}_f^{meas}|$  (blue), in panel (b).

Figure 4(a) shows how the total power of the difference depends on  $\gamma$ . The graph is an almost-perfect parabola, which can be appreciated by considering the curve below the horizontal grey dashed line at  $50.10 \text{ mm}^2 \text{ s}$ , which is the (approximate) value of  $E(u - u^{meas})$ , given by  $E(u_\gamma - u^{meas})$  at  $\gamma = 0$ ; the integral norm of the difference with a quadratic fit is of order  $O(10^{-2})$ . This suggests again that the correction as given in Equation (2) is of first order. Figure 4(b) and (c) show the resulting relative displacement from Equation (2) with  $\gamma = 0$ , that is, the result obtained from Equation (1), and  $\gamma = 0.452$ , which is the location of the approximate minimum  $\gamma^*$ , respectively; the grey time series in the background is the measured displacement  $u^{meas}$ . The total power of the difference between computed and measured displacements has reduced to approximately  $24.44 \text{ mm}^2 \text{ s}$  at the optimal value  $\gamma = \gamma^*$ .

Figure 5 shows these results in the frequency domain. Panel (a) shows the Fourier amplitudes  $|(\hat{u}_{\gamma^*})_f|$  and  $|\hat{u}_f|$  of the computed displacements  $u_{\gamma^*}$  and  $u$ , that is the generated response from Equation (2) with  $\gamma = \gamma^*$  and  $\gamma = 0$ , respectively; here  $|(\hat{u}_{\gamma^*})_f|$  is coloured teal and  $|\hat{u}_f|$  is blue. Note the linear property of this correction: each frequency satisfies

$$|(\hat{u}_{\gamma^*})_f| \leq K |\hat{u}_f|,$$

where the constant  $K = 1 - \gamma^*$  is indeed found to be approximately  $K = 0.548$ .

Figure 5(b) shows the power spectrum of the difference with  $u^{meas}$ , again for  $(\hat{u}_{\gamma^*})_f$  (teal) and  $\hat{u}_f$  (blue). The effect of the linear correction is a sharpening of the power spectrum, with the maximum achieved at the sampling point  $f = 47/24 \approx 1.96 \text{ Hz}$ , closest



to the fundamental frequency for both computed displacements; the values of the peaks are 10.65 mm s for  $(\hat{u}_{\gamma^*})_f$  and 10.24 mm s for  $\hat{u}_f$ .

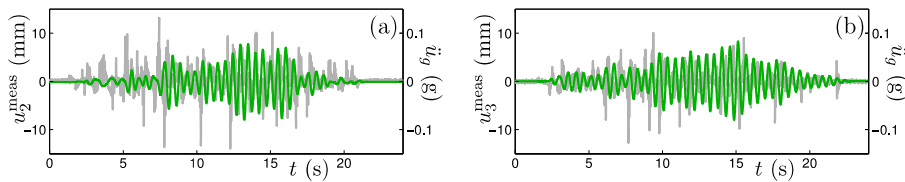


Figure 6: Measured relative displacements, each shown with the applied ground acceleration, for the other two experiments, where the main frequency of the applied ground acceleration lies increasingly closer to the fundamental frequency of the SDOF structure; compare with Figure 2(a).

The experiment was repeated with two other ground accelerations that have main frequencies increasingly closer to the fundamental frequency of the SDOF structure. Figure 6 shows the measurements from these two additional experiments. Panel (a) shows the measured relative displacement  $u_2^{meas}$  overlaid on the associated ground acceleration, which corresponds to the vertical axis on the right. Panel (b) shows the same plot for the measured relative displacement  $u_3^{meas}$  associated with the third experiment. The same comparisons and corrections were made for these two additional data sets.

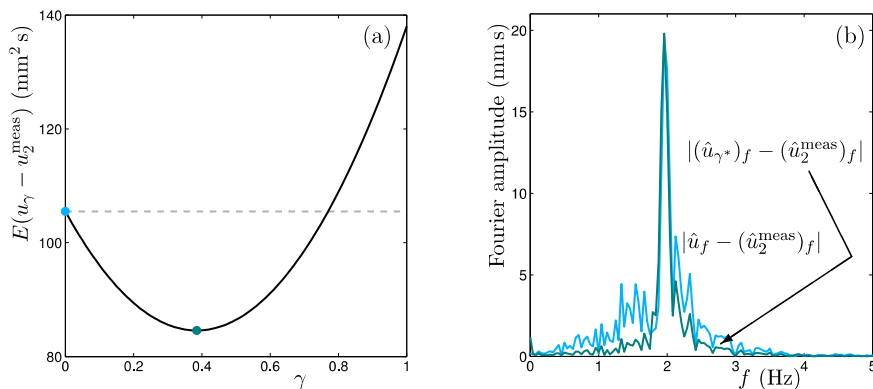


Figure 7: Results for the response generated from Equation (2) with the load as in the second experiment. Panel (a) shows the total power of the difference with  $u_2^{meas}$  as a function of  $\gamma$ , and panel (b) shows the corresponding power spectra for the cases  $\gamma = 0$  (blue) and  $\gamma = \gamma^* \approx 0.385$  (teal); compare with Figure 5.

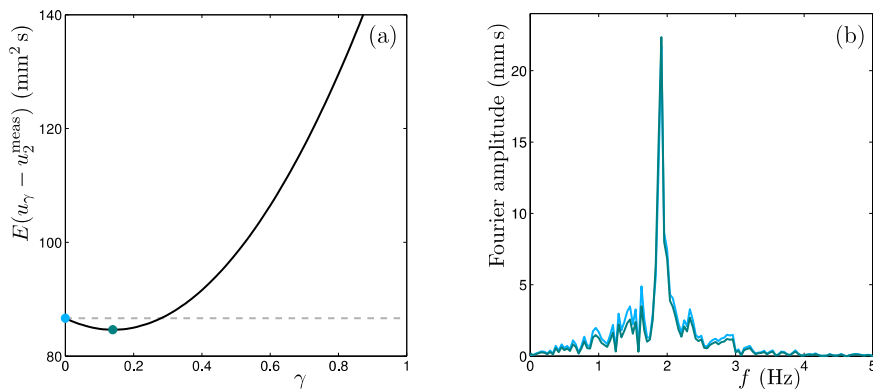


Figure 8: Results for the response generated from Equation (2) with the load as in the third experiment. Panel (a) shows the total power of the difference with  $u_3^{meas}$  as a function of  $\gamma$ , and panel (b) shows the corresponding power spectra for the cases  $\gamma = 0$  (blue) and  $\gamma = \gamma^* \approx 0.139$  (teal), which lie practically on top of each other; compare with Figures 5 and 7.

Figure 7 shows the results for the experiment associated with  $u_2^{meas}$ . As for the first experiment, Equations (1) and (2) were used to generate computed displacements. Panel (a) shows the total power of the difference between the displacement  $u_\gamma$  generated from Equation (2) and  $u_2^{meas}$  as a function of the correction  $\gamma$ . As before, the graph is parabolic with a well-defined minimum; the optimal correction for this case is to adjust the load by a factor  $1 - \gamma^*$  with  $\gamma^* \approx 0.385$ . Panel (b) shows the power spectrum of the difference with  $u_2^{meas}$  for the responses  $u_\gamma$  with  $\gamma = 0$  (blue), which is the same as the response generated from Equation (1), and with  $\gamma = \gamma^*$  (teal).



Similarly, Figure 8 shows the results for the experiment associated with  $u_3^{meas}$ . Again, Equations (1) and (2) were used to generate computed displacements. Panel (a) illustrates the parabolic nature of the total power of the difference between the displacement  $u_\gamma$  generated from Equation (2) and  $u_3^{meas}$  as a function of  $\gamma$ . The minimum occurs at  $\gamma^* \approx 0.139$ . Panel (b) shows the power spectrum of the difference with  $u_3^{meas}$  for the responses  $u_\gamma$  with  $\gamma = 0$  (blue), which is again the same as the response generated from Equation (1), and with  $\gamma = \gamma^*$  (teal). The main frequency of the ground acceleration for this third experiment is approximately the same as the fundamental frequency of the SDOF structure. Consequently, the correction from Equation (2) has very little effect and the two curves in Figure 8(b) almost lie on top of each other. Indeed, as can be seen in Figure 8(a), the minimum at  $\gamma^*$  lies very close to 0 and the reduction of the total power  $E(u_\gamma - u_3^{meas})$  is only from  $86.67 \text{ mm}^2 \text{ s}$  at  $\gamma = 0$  to  $84.65 \text{ mm}^2 \text{ s}$  at  $\gamma^* = 0.139$ .

## 4 CONCLUSIONS

Three different ground accelerations were considered to study how well the relative displacement calculated from the conventional harmonic equation matches the measured relative displacement. The results indicated that the discrepancy is of first order, that is, this linear equation appears not to take into account linear effects. We tested the hypothesis that the load experienced by the SDOF structure is actually different from the load generated by the ground acceleration.

This investigation led to the following conclusions:

1. A linear correction of the form

$$m \ddot{u} + c \dot{u} + k u = -(1 - \gamma) P(t),$$

as given in Equation (2), can lead to an improvement in terms of the total power  $E(u_\gamma - u^{meas})$  of the difference with the measured response. Here, the response  $u$  obtained from the conventional harmonic equation is the same as the response  $u_\gamma$  with  $\gamma = 0$ .

2. The corrected response  $u_\gamma$  satisfies

$$u_\gamma = (1 - \gamma) u,$$

but the total power  $E(u_\gamma - u^{meas})$  does not depend linearly on  $\gamma$ .

3. There exists an optimal value  $\gamma^*$  for which  $E(u_\gamma - u^{meas})$  is minimal. In fact,  $E(u_\gamma - u^{meas}) < E(u - u^{meas})$  as soon as  $\gamma > 0$  up to a certain maximum that is approximately equal to  $2\gamma^*$ , that is,  $\gamma^*$  lies approximately at the midpoint of the  $\gamma$ -interval for which  $E(u_\gamma - u^{meas}) < E(u - u^{meas})$ .
4. Unfortunately,  $\gamma^*$  depends on the ground acceleration. It seems that  $\gamma^* \rightarrow 0$  in the limit as the main frequency of the ground acceleration moves towards the fundamental frequency of the SDOF structure.

An important observation is that the relative displacements generated from the equations of motion are larger than those measured in the experiments. In contrast, the findings in (Qin et al., 2018) suggest that Equation (1) generates a smaller relative displacement if the ground acceleration is a pure sine wave. However, similar to what is observed here, the results reported in (Qin et al., 2018) also show a significant discrepancy centred at the fundamental frequency of the SDOF structure.

## ACKNOWLEDGEMENTS

This research was supported by grant #3712132 from the Engineering Faculty Research Development Fund of the University of Auckland.

## REFERENCES

- Chopra, A.K. 2001. *Dynamics of Structures: Theory and Applications to Earthquake Engineering*. 2nd ed., Upper Saddle River, NJ: Prentice-Hall.
- Chow, N., Orense, R. & Larkin, T. (ed.). *Seismic Performance of Soil-Foundation-Structure Systems*. London: CRC Press. 123–136.
- Chow, N. 1996. Effect of the earthquake on 17<sup>th</sup> of January 1995 on Kobe, *Proceedings of the D-A-CH meeting of the German, Austrian and Swiss Society for Earthquake Engineering and Structural Dynamics*, University of Graz, Austria, 135–169.
- Chow, N. & Hao, H. 2012. Pounding damage to buildings and bridges in the 22 February 2011 Christchurch earthquake, *International Journal of Protective Structures*, Vol 3(2), 123–139.
- Chow, N., Orense, R. & Larkin, T. 2017. *Seismic Performance of Soil-Foundation-Structure Systems*. London: CRC Press.
- Crisp, J.D.C., Ryall, T.G. & D’Cruz, J. 1990. Determining a force acting on a plate — An inverse problem, *AIAA Journal*, Vol 29(3), 464–470.



- Kawashima, K., Unjoh, S., Hoshikuma, J.I. & Kosa, K. 2011. Damage of bridges due to the 2010 Maule, Chile, earthquake, *Journal of Earthquake Engineering*, Vol 15(7), 1036–1068.
- Orense, R., Towhata, I. & Chouw, N. 2014. *Soil Liquefaction during Recent Large-Scale Earthquakes*. London: CRC Press.
- Qin, X., Xu, H., Chouw, N., Larkin, T. & Osinga, H.M. 2018. Shake table simulation of dynamic forces of a structure, *Proceedings of the New Zealand Society for Earthquake Engineering*, Auckland, 2018.
- Takewaki, I. & Kojima, K. 2017. Double, triple and multiple impulses for critical elastic-plastic earth quake response analysis to near-fault and long-duration ground motions.

